Solid Earth Discuss., 6, 403–426, 2014
www.solid-earth-discuss.net/6/403/2014/
doi:10.5194/sed-6-403-2014

Solid Earth
Discussions
Open Access

Crustal heat flow measurements in western Anatolia from borehole equilibrium temperatures

K. Erkan

Department of Civil Engineering, Faculty of Engineering, Marmara University, 34722, Göztepe, Istanbul, Turkey

Received: 7 January 2014 – Accepted: 16 January 2014 – Published: 30 January 2014

Correspondence to: K. Erkan (kamil.erkan@marmara.edu.tr)

Published by Copernicus Publications on behalf of the European Geosciences Union.

Abstract

Results of a crustal heat flow analysis in western Anatolia based on borehole equilibrium temperatures and rock thermal conductivity data are reported. The dataset comprises 113 borehole sites that were collected in Southern Marmara and Aegean regions of Turkey in 1995–1999. The measurements are from abandoned water wells with depths of 100–150 m. Data were first classed in terms of quality, and the low quality data, including data showing effects of hydrologic disturbances on temperatures, were eliminated. For the remaining 34 sites, one meter resolution temperature-depth curves were carefully analyzed for determination of the background geothermal gradients, and any effects of terrain topography and intra-borehole fluid flow were corrected when necessary. Thermal conductivities were determined either by direct measurements on representative surface outcrop or estimated from the borehole lithologic records. The calculated heat flow values are 85–90 mW m^{-2} in the northern and central parts of the Menderes horst-graben system. Within the system, the highest heat flow values (> 100 mW m^{-2}) are observed in the northeastern part of Gediz Graben, near Kula active volcanic center. The calculated heat flow values are also in agreement with the results of studies on the maximum depth of seismicity in the region. In the Menderes horst-graben system, surface heat flow is expected to show significant variations as a result of active sedimentation and thermal refraction in grabens, and active erosion on horst detachment zones. High heat flow values (90–100 mW m^{-2}) are also observed in the peninsular (western) part of Çanakkale province. The heat flow anomaly here may be an extension of the high heat flow zone previously observed in the northern Aegean Sea. Moderate heat flow values (60–70 mW m^{-2}) are observed in eastern part of Çanakkale and central part of Balıkesir provinces.

SED
6, 403–426, 2014

1 Introduction

Determination of the crustal heat flow has many important applications including understanding recent to present-day plate tectonic activity (Blackwell et al., 1991; Erkan and Blackwell, 2008, 2009), maximum depth of seismicity (Bonner et al., 2003), and understanding geothermal energy potential of an area (Tester et al., 2006). The conventional techniques for determinations of regional heat flow on land involve measurement of equilibrium rock temperatures as a function of depth in boreholes, and determination of rock thermal conductivity at the same location of the borehole (Beardsmore and Cull, 2001). Temperature gradients must be processed and corrected for various effects including terrain topography, intra-borehole fluid flow, microclimate, etc. (Jaeger, 1965; Roy et al., 1972). Such analyses require availability of high-resolution equilibrium temperature data from boreholes of sufficient depths (> 100 m).

Previously, the regional heat flow map of western Anatolia was published as part of the heat flow map of Turkey (Tezcan and Turgay, 1991). This map uses bottom-hole temperature (BHT) data from 204 deep oil/gas wells, as well as data from geothermal exploration wells that are not under the influence of local geothermal activity. After temperatures were corrected for drilling fluid circulations, a constant thermal conductivity of 2.1 $W m^{-1} K^{-1}$ was assumed for calculation of conductive heat flow. Calculated heat flow values were > 100 $mW m^{-2}$ for the southwestern part of the Marmara and major parts of the Aegean regions. In Turkey, heat flow determinations using the conventional techniques have been very limited. In the Marmara region, Pfister et al. (1998) reported crustal heat flow values using temperature-depth data from unused water wells and thermal conductivities from surface outcrops. They report a mean crustal heat flow of 75 $mW m^{-2}$ for the Southern Marmara region.

In Turkey, between 1995 and 1999, a major campaign of temperature-depth and thermal conductivity measurements was carried out under two government-funded projects (İlkışık et al., 1996, 1997). The dataset has not been analyzed before using conventional heat flow determination techniques. In this study, the results of the analysis of

SED
6, 403–426, 2014

this dataset are reported for western Anatolia, which includes Southern Marmara and Aegean regions.

2 Data collection strategy

The data collection was realized by General Directorate of Mineral Research and Exploration (MTA) under the leadership of H. M. Yenigün (personal communication, 2012). Boreholes are owned and operated by the State Hydrological Affairs (DSI) and Rural Services (presently, out of service) regional offices. These boreholes were either drilled as water supply wells (but not producing) or as groundwater monitoring wells. For each borehole site, lithologic information from drillers, and other useful data (e.g. well depth, static level, etc.) were obtained from the personnel of the state agencies. The wells are generally cased for their entire depth and are perforated at certain levels.

Temperature-depth (T-D) measurements were made by a surface-read out portable temperature logging tool. Static water levels were determined before each measurement using a sinker, and temperatures were measured from the bottom-to-top at a 1 m interval. For thermal conductivity measurements, surface rocks samples were collected from outcrops in the vicinity of each measurement site ($\sim$ 500 m in radius). Thermal conductivity measurement were made using QTM-500 needle probe tool. Generally, more than one type of lithology was sampled resulting in a larger dataset for rock thermal conductivities. A statistical analysis of these thermal conductivity measurements is given by Balkan et al. (2014).

3 Quality classification

In crustal heat flow determinations, the instrumental (random) error originating from the sampling of formation temperatures and rock thermal conductivities are negligibly small (Blackwell and Spafford, 1987). On the other hand, major uncertainties in heat flow determinations are related to the actual physical condition of the measurement site including well depth, local and regional hydrologic effects, and the quality of the thermal conductivity determinations. The quality of a heat flow determination is given by a combination of these different conditions. In practice, data are divided in different quality classes and codes, according to these parameters. For reference, details of the data classification strategy are discussed below.

Contribution of the subsurface hydrologic activity (convection) on formation temperatures can be determined by a detailed analysis of the temperature-depth (T-D) curves. To determine the points showing conductive heat transfer, the solution of the one-dimensional heat conduction equation is enforced on the measured T-D curves (Jaeger, 1965; Roy et al., 1972; Beardsmore and Cull, 2001). Firstly, in a subsurface medium with uniform thermal conduction, the one-dimensional steady-state heat conductive equation requires a linearly increasing T-D curve. Secondly, the (extrapolated) value of the subsurface temperatures at $z = 0$ (surface boundary condition) must match the mean annual surface temperature (MAST) of the measurement point. The MAST values can be independently obtained from meteorological records and models. These conditions are strictly enforced on the measured T-D data to understand whether the site is under a conductive or convective thermal regime. However, a high resolution T-D dataset is required in order to make such an analysis.

Förster and Smith (1989) show that for rock permeability values below 10^{-18} m^2 heat transfer is controlled by conduction, and for permeability values above 10^{-15} m^2, heat transfer is controlled by convection. Between these regimes, both conductive and convective heat transfer have an effect on subsurface thermal conditions. Their results give a qualitative approach which returns a yes/no type solution for conductive/convective heat transfer at the data location. Alternatively, a quantitative approach can be used by modeling the subsurface hydrologic conditions (see Pfister et al., 1998). However, this modeling approach may not be reliable due to ambiguities of the subsurface geologic and hydrologic conditions. So, a more conservative approach of using data only under conductive thermal regime is followed here. Meanwhile, the results can also be used to understand the subsurface permeability conditions of the measurements site.

SED
6, 403–426, 2014

A common hydrologic activity observed on borehole T-D profiles is intra-borehole fluid flow (Roy et al., 1972; Erkan et al., 2008). For holes that are not grouted, this occurs as a result of hydrologic shortcuts between different pressure regimes at different structural horizons. In this case, the fluid moves up or down from high to low pressure regimes. This is a local hydrologic phenomenon that occurs within the borehole, and does not represent the thermal conditions of the subsurface medium. In these wells, background thermal conditions can be recovered if the entire borehole temperatures are not overprinted by fluid flow. On T-D curves, intra-borehole flow activity is easily detected by sharp changes where the fluid enters and exits the borehole. An upflow results in higher than normal (background) temperatures whereas a downflow causes a lower than normal (background) temperatures. In the present dataset, many wells were observed to show these effects. Although intra-borehole flow can be corrected in most cases, it introduces an uncertainty in gradient calculations, hence larger uncertainty in heat flow determinations.

Rock thermal conductivity is a principal component of heat flow determinations, and therefore needs to be quantified as accurately as possible. For example, an error of 0.25 $\mathrm{W\,m^{-1}\,K^{-1}}$ in the thermal conductivity value results in 10 $\mathrm{mW\,m^{-2}}$ (12.5 %) error in heat flow (assuming a temperature gradient of 40 °C $\mathrm{km^{-1}}$ and heat flow of 80 $\mathrm{mW\,m^{-2}}$). The primary method of thermal conductivity measurement is on whole core samples from the lithologic sections present in each borehole but these samples are usually not available; so, secondary methods are used. These include measurements on drill cuttings (if available), measurements on outcrops that represent the subsurface lithology, or by assigning a value from literature based on the lithologic records of the borehole. The subsequent error in thermal conductivity determination depends on the method used.

The classification scheme used in this study is adopted from Blackwell et al. (1982, 1990). According to this, Class A type data (5 % error in heat flow values) have at least a 100 m linear T-D section and thermal conductivity measurements made on core samples. Class B type data (10 % error in heat flow values) must have at least a 50 m

Discussion Paper | Discussion Paper | Discussion Paper | Discussion Paper |

SED
6, 403–426, 2014

Title Page
Abstract Introduction
Conclusions References
Tables Figures
◀| |▶
◀ ▶
Back Close
Full Screen / Esc
Printer-friendly Version
Interactive Discussion

linear T-D section, and some measurements of thermal conductivity (measurements on core samples, drill cuts, data from nearby wells, representative outcrop samples, etc.). Data is in Class C (25 % error in heat flow values) if gradients are disturbed by intra-borehole fluid flow, and some thermal conductivity is information is available. If no thermal conductivity information is available heat flow cannot be determined, and data is in Class D. This class of data is useful for their gradient information. The remaining classes of data are the ones showing hydrologic effects. Holes under the influence of geothermal activity are assigned Class G (geothermal system), and holes showing the effect of regional groundwater activity are assigned Class X. For crustal heat flow analysis, data in classes of A, B, or C are required.

The quality classification scheme mentioned above was applied for the data in the study area. The distribution of data with quality classes are shown in Fig. 1. No Class A type data are available due to unavailability of rock core samples. Data quality show an interesting geographic dependence. In provinces such as Çanakkale (CAN), İzmir (IZM), and Manisa (MAN), good quality (B/C) data are generally encountered. On the other hand, all of the data collected in provinces such as Afyon (AFY), Denizli (DEN), Muğla (MUG) show convective behavior, and not suitable for regional heat flow analysis. Class D type data in Uşak (USA) and Kütahya (KUT) provinces are due to limitations in thermal conductivity determinations in these area. Though, holes in these locations show conductive behavior.

4 Data analysis

During analysis of T-D curves, data for each province were combined into a single plot, thereby enabling correlations between different T-D curves for the same province. That is, data in conductive thermal regimes show similar behavior, and differences are mostly related to thermal conductivity variations, or differences in MAST values; within a single province, MAST values mainly depend on the elevation of the data points. On the other hand, data showing convective behavior show complex and usually dis-

SED
6, 403–426, 2014

tinctly different behavior compare to data showing conductive behavior. In the following paragraphs, T-D curves for B and C classes of data for each province are discussed (Fig. 2).

In Çanakkale (CAN) (Fig. 2a), T-D curves show generally conductive behavior, and intra-borehole fluid disturbances are minimal. Inferred background temperature profiles are shown by dashed lines in the figure. For Pazarkoy, a weak downflow is observed between 33–55 m, and for Cavuskoy, a strong upward flow between 95–125 m is apparent. Also for Yapildak, a strong upflow from 25 m up to the surface is apparent. Projected MAST values (value of dashed lines at $z = 0$) can be correlated with the elevations of the data points (see Table 1 for elevation of each data point). An adiabatic lapse rate of $\sim 5\,^{\circ}\mathrm{C\,km^{-1}}$ for air mass may be used for comparing MAST values at different elevations. Intepe has the lowest elevation and is located near the shoreline, and it shows the highest MAST value. Cavuskoy is also at low elevation but is slightly inland, so MAST value is slightly lower. On the other hand, Pazarkoy and Terzialan are located inland at higher elevations, and they have even lower MAST values. Interestingly, for Yapildak the projected MAST value is very low even though it is near Intepe. For this well, a downflow must be occurring for a long time period so that $z = 25$ m acts as the apparent surface for the well. Below this depth, gradients represent a conductive thermal regime. Also of note, the sharp break in gradient at 65 m for Intepe is interesting. The lithologic records indicate a change from mudstone to diabase at $z = 86$ m. The sharp break in gradients must be related to this lithologic change because thermal conductivity of the mudstone is ($\sim 1\,\mathrm{W\,m^{-1}\,K^{-1}}$) distinctly different from diabase ($\sim 2\,\mathrm{W\,m^{-1}\,K^{-1}}$). The Yapildak well also penetrates a mudstone lithology at depths of 40–80 m, and shows similar gradients of the mudstone lithology at Intepe (Table 1).

In Fig. 2b, T-D curves for Bursa (BUR) and Balıkesir (BAL) provinces are shown along with interpreted background temperatures (dashed lines). In general, T-D curves show high degree of disturbance due to intra-borehole fluid flow at multiple depths. Nevertheless, background gradients can be estimated from the conductive sections.

SED
6, 403–426, 2014

Extrapolated MAST values are similar for all data, and in agreement with meteorological records (Fig. 1, values in blue boxes).

T-D curves for Izmir (IZM) province are shown in Fig. 2c. In general, data appear to be of excellent quality with no indication of major hydrologic disturbance. For Yusufdere, the first 50 m of the well show nearly isothermal behavior, but below this depth a conductive regime is apparent. Two wells in the peninsular region (Ciftlikkoy and Ovacıki) have the highest MAST values compare to the other wells that are inland. These two wells penetrate a similar (marl) lithology for the entire section and also show similar gradients. The Bademli well penetrates a very high conductivity sandstone section (Table 1), which may be responsible for the low gradient in this well. Another interesting feature in certain wells in Fig. 2c is the systematic curvatures at 0–50 m interval toward higher temperatures. The exact cause of these systematic deviations is not clear at this point; they may be related to some microclimatic conditions at the surface, or to transient changes in MAST values.

T-D curves for the Manisa (MAN) province are shown in Fig. 2d. Although data show some local fluctuations, they generally represent the conductive background thermal regime, and effect of intra-borehole flow is minor. These fluctuations in the data may be related to disturbance of the equilibrium thermal conditions during logging, and emergence of cellular convections inside the well (Sammel, 1968). This may also explain the lack of fluctuations at 53–85 m interval of Cataloluk. Lithologic reports show that the well penetrates a marl lithology between 0–53 m, a tuff lithology between 53–85 m, and a sandstone lithology below this depth. If the tuff section here is young and permeable, the hydrologic activity in this section may have destroyed the small convection cells.

SED
6, 403–426, 2014

5 Results

For classes B, C, and D type data, detailed well information, and the calculated heat flow values are tabulated in Table 1. The final heat flow values (Q) were determined after additional corrections which are discussed below.

3-D visualization of the geographic setting of each well site (geology, topography, proximity to urban areas, etc.) was made possible by transferring the data in Google Earth software (http://www.google.com/earth/). For some wells, topographic corrections on the gradients were necessary. For this purpose, a 2-D analytical model (Lee's topographic correction, see Jaeger, 1965; Beardsmore and Cull, 2001) was used. In this model, the topography is fitted to a two-dimensional hill or a monocline of a certain height and width. The width and height information can easily be obtained using the Elevation Profile module of Google Earth. Topographic corrections resulted in up to 10 °C km^{-1} difference in gradients (Table 1). The error from the assumption of 2-D topography in this correction is expected to be within the general error limit of the data (i.e., 10 % for Class B, and 25 % for Class C).

Thermal conductivities were determined based on the lithology of the interval where the gradients were calculated. For measured thermal conductivities (indicated as M next to the value), a correction for porosity was applied from natural to water-saturated conditions (Balkan et al., 2014). If no measurement is available, the thermal conductivity was assigned from the literature (indicated as L next to the value) based on the reported lithology of the interval. For all data points located in quaternary basins, a generic value of 1.5 W m^{-1} K^{-1} was used (Blackwell, 1983).

For mapping the regional distribution of the heat flow data, the results of this study (İlkışık data, 34 data points) were combined with the results of Pfister et al. (1998) (Pfister data, 26 data points). For the Pfister data, a conservative approach was used, and values outside of the 40–140 mW m^{-2} range were eliminated due to possible hydrological disturbances. The resulting heat flow map is shown in Fig. 3. The southern part of Aegean region is not covered on the map due to the lack of good quality (B, C, D) heat flow data there. For mapping purposes, Class D data in Kütahya (KUT) and Uşak (USA) provinces were also added by assigning a generic thermal conductivity value of $2.0\,\mathrm{W\,m^{-1}\,K^{-1}}$ (based on the general geology of these regions). However, the map in these provinces has unknown reliability.

In generating the heat flow map in Fig. 3, further corrections were applied to three points (Yenmis, Yusufdere, and Alasehir) in alluvial fans of the Menderes graben system. Details of these corrections are discussed in the following section.

6 Heat flow in Menderes horst-graben system

The general tectonic setting of the area of interest in this paper is extensional (Bozkurt, 2001; Aktug et al., 2009). Within the general study area, Menderes horst-graben system (blue dashed lines in Fig. 3; also called Menderes Crystalline Core Complex, or Menderes Massif) shows the most pronounced features of an active extensional system. As shown in Fig. 3, the area can be divided into three major horst units of Northern Menderes Unit (NMU), Central Menderes Unit (CMU), and Southern Menderes Unit (SMU), separated by two major grabens units of Gediz Graben (GG) and Büyük Menderes Graben (BMG). Mechanisms affecting surface heat flow distribution in extensional regions are discussed in detail by Blackwell (1983). The most significant ones are the effects of active sedimentation and erosion, thermal refraction from the basins, and variations of radioactive heat production in rocks. Below, expected contributions of these effects are discussed for the Menderes horst-graben system.

6.1 Erosion and sedimentation

In tectonically active areas, active sedimentation and erosion have an effect on surface heat flow (Jaeger, 1965; Beardsmore and Cull, 2001). In areas under active erosion, crustal geotherms are moved toward the surface which results in higher heat flow values near the surface. On the other hand, in areas of active sedimentation, geotherms

SED
6, 403–426, 2014

are moved down resulting in lower heat flow near the surface (also called thermal blanketing). Results of these effects on measured (surface) heat flow are shown in Fig. 4, as a function of rates of erosion and deposition. The results in Fig. 4 are shown for erosional/depositional activity for the last 5 Myr, and crustal heat flow of 85 $mW m^{-2}$.

Erosional history of a region can be estimated by studying time-versus-temperature tracks provided by radiometric dating and fission-track techniques. Gessner et al. (2001) and Ring et al. (2003) report the cooling history of different parts of the Menderes core complex using fission-track and Ar-Ar dating methods (also see Seyitoğlu et al., 2004, for a review). These studies show an early phase of significant cooling during Late Oligocene and Early Miocene in the northern (NMU) and southern (SMU) Menderes Units, but present-day erosion rates are minimal in these regions. On the other hand, the Central Menderes Unit (CMU) has experienced cooling in Pliocene to the recent. These studies report that northern and southern edges (called detachments) of the CMU have been experiencing a rapid present-day cooling. The cooling rates are estimated to be $\sim 50\,^{\circ}C\,km^{-1}$ for the last 5 Myr (Gessner et al., 2001) which imply erosion rates of $\sim 1000\,m\,Myr^{-1}$. If so, apparent heat flow on these detachment zones must be $> 250\,mW\,m^{-2}$ (see Fig. 4a). However, there is currently no data point on these detachment zones to verify this hypothesis.

Present-day deposition rates inside the grabens can be quantified from sedimentological records. The studies show that modern Gediz graben is Plio-Quaternary ($\sim$ 5 Myr) in age (Koçyiğit et al., 1999; Bozkurt and Sözbilir, 2004). The thickness of the sediments accumulated during this time interval has a range of 200–1000 m (Seyitoğlu and Scott, 1996; Bozkurt and Sözbilir, 2004; Çiftci and Bozkurt, 2010) depending on the location. These depositional rates of 40–200 $m\,Myr^{-1}$ correspond to surface heat flow values of 5–20 $mW\,m^{-2}$ lower than the crustal values (Fig. 4b). The actual difference depends on the location where the heat flow is measured. Largest variations are expected to occur for boreholes located in alluvial fan deposits, where the highest regional rates of deposition take place. In the present dataset (Table 1), three sites

SED
6, 403–426, 2014

(Yenmis, Yusufdere, and Alasehir) are located on alluvial fan deposits in this area, and a constant correction of +20 $mW\,m^{-2}$ was applied to these points.

6.2 Thermal refraction

In areas with significant lateral variations of thermal conductivity, crustal heat flow is refracted from lower conductivity to higher conductivity areas. This phenomenon most dramatically occurs in horst-graben systems as a result of the large contrast between thermal conductivity of ranges (horsts) and basins (grabens). Thakur et al. (2012) studied this effect by using a 3-D model for Dixie Valley in Nevada (USA), which has a similar geometry to Gediz graben in Turkey. For a background heat flow of 90 $mW\,m^{-2}$, they calculated surface heat flow of ~ 75 $mW\,m^{-2}$ inside the graben, that is ~ 15 $mW\,m^{-2}$ below the background heat flow. On the other hand, heat flow values of ~ 120 $mW\,m^{-2}$ were observed for parts of the ranges adjacent to the graben. Within internal parts of the ranges, surface heat flow values are similar to the crustal values. A similar type of behavior for thermal refraction may be expected for Menderes horst-graben system. In this dataset (Table 1), the three data points on the alluvial fan deposits are expected to be affected by the thermal refraction, thus a further correction of +10 $mW\,m^{-2}$ was applied to these points (Fig. 4).

6.3 Radiogenic heat production

Another important contribution on the surface heat flow comes from the heat production of radioactive elements (U, Th, K) in the upper crustal rocks. On average, upper crustal rocks have heat production values of 2–3 $\mu W\,m^{-3}$ which corresponds to about 20–30 $mW\,m^{-2}$ of total surface heat flow (Blackwell, 1983). Significantly higher heat flow values are expected for data measured on felsic intrusive rocks (e.g., granite, 4–5 $\mu W\,m^{-3}$), and metamorphic rocks that are derived from these felsic intrusives (e.g., gneiss) (Wollenberg and Smith, 1987). Among sedimentary rocks, shale shows radioactivity values equivalent to granite; other sedimentary rocks have low to moderate

SED
6, 403–426, 2014

heat production values (Wollenberg and Smith, 1987). In the study area, the most interesting rock types in terms of radioactivity are exposed units of the Menderes metamorphic core complex. Glodny and Hetzel (2007) reports U content of granitic rocks sampled from the northern part of the Central Menderes unit (Turgutlu and Salihli granitoids). They report U content of 1.1 ppm which corresponds to a heat production value of $\sim 1.5\,\mu\mathrm{W\,m^{-3}}$. If this value is representative of the core complex, radiogenic heat production is not a strong contributor to the regional heat flow distribution. However, more measurements from different parts of the core complex are needed for a more definitive statement.

7 Discussion

In the Menderes horst-graben system, average heat flow is 85–90 $\mathrm{mW\,m^{-2}}$, and becomes $> 100\,\mathrm{mW\,m^{-2}}$ in the northeastern part of Gediz graben. This is also the only area in the study region where holocene volcanic activity has been occurring (Kula volcanic field; Fytikas et al., 1984; shown as purple triangle in Fig. 3). Heat flow reported in this study is somewhat lower than values reported by Tezcan and Turgay (1991), which are $> 100\,\mathrm{mW\,m^{-2}}$ in most parts of the Menderes system. The values reported in this study are based on direct sampling of borehole equilibrium temperatures and thermal conductivities, so they are expected to be more reliable.

The heat flow map in Fig. 3 can be compared independently by maximum depth of seismicity (Bonner et al., 2003; Erkan and Blackwell, 2009). This is because maximum depth of seismicity is directly related to the crustal temperatures in a region. However, high quality (less than ~ 2 km depth error) hypocenter data are required to make this analysis. Such high quality hypocenter data were reported by Akyol et al. (2006) across the Menderes horst-graben system. For their class A events, the maximum depths of seismicity are between 13–15 km in the central part of CMU (Fig. 3) and as deep as 20 km in the eastern part of CMU. Comparing the results of Bonner et al. (2003) and Erkan and Blackwell (2009) in western North America, these depths corresponds to

SED
6, 403–426, 2014

Title Page
Abstract | Introduction
Conclusions | References
Tables | Figures
◀◀ | ▶▶
◀ | ▶
Back | Close
Full Screen / Esc
Printer-friendly Version
Interactive Discussion

heat flow values of 75–90 mW m^{-2}, and are in general agreement with the result of this study. Another high-resolution survey is reported by Aktar et al. (2007) on the peninsular region of Izmir. Two class-B heat flow data (Ciftlikkoy and Ovaciki, Table 1) show heat flow values of 85–86 in this region. Aktar et al. (2007) recorded events down to $\sim$ 13 km (taking a 95 % confidence interval) which are also in agreement with the reported heat flow values.

Heat flow values of 90–100 mW m^{-2} are observed in the peninsular part of Çanakkale (Fig. 3). The high heat flow here may be the extension of the high heat flow (Jongsma, 1974) and low *P* wave seismic velocity zone (Piromallo and Morelli, 2003) observed in the Northern Aegean Sea. In the eastern part of Çanakkale and central part of Balıkesir, a region of moderate heat flow values (65–70 mW m^{-2}) is constrained by both Pfister and Ilkisik data. Moderate values in Balıkesir are also shown on the map of Tezcan and Turgay (1991). In Çanakkale, data points are located in quaternary sediments, and at least part of the low values may be related to near-surface effects. Relatively low heat flow values in the central part of Balıkesir are mostly controlled by Pfister data, and currently unexplained. Since the area is located on the Miocene age Edremit Graben, one possibility is the low radiogenic heat production of rocks in this area.

8 Conclusions

In this study, new crustal heat flow values for western Anatolia are reported based on equilibrium borehole temperatures and thermal conductivity data. The data were first separated in different quality classes, and sites showing conductive heat transfer were selected by applying the principles of 1-D conductive heat transfer. For 34 Class B/C/D quality sites, geothermal gradients were evaluated by a detailed analysis of temperature-depth curves. Conventional correction procedures including intra-borehole flow, and terrain effects were applied to the gradients. Thermal conductivities were either measured from outcrop samples or generically determined based on litho-

SED
6, 403–426, 2014

logic information from driller reports. Using the calculated heat flow data in the study and data reported from the earlier studies, a regional heat flow map of the region is generated. For Menderes extensional region, heat flow is calculated to be 85–90 mW m^{-2}, with values > 100 mW m^{-2} in the northeastern part of Gediz Graben. Another high heat flow region is observed in the peninsular region of Çanakkale (90–100 mW m^{-2}). For Menderes horst-graben system, present-day erosion/sedimentation activity, and the thermal refraction in the basins can have a significant influence on the surface heat flow. The magnitude of these effects depends on the conditions of the specific measurement site.

Acknowledgements. The author is indebted to M. İlkışık for providing the field data, which enabled the realization of this study. The author would like to thank S. Ergintav and S. İnan for their support in this research while he was a visiting scholar at Marmara Research Center. This study was supported by TÜBITAK BIDEB 2232 program, and Marmara University, Scientific Research Commission (FEN-A-100413-0127). Travel support for this project was provided by Marmara University, Scientific Research Commission (FEN-D-130313-0093). The author would also like to thank V. Ediger, B. Erkan, and C. Tapırdamaz (Marmara Research Center) for providing some useful data and software tools. The database of hot springs was obtained from ATAG Earth Sciences Catalog (Coordinator: M. C. Tapırdamaz). The manuscript was greatly improved by constructive reviews of M. Ilkışık (Anadolu Geosciences), and M. Richards, Z. Frone, R. Dingwall, and C. Mauroner (SMU Geothermal Laboratory). Some of the heat flow data processing was performed using the modules of G. R. Beardsmore at Monash University (http://monash.edu/science/about/schools/geosciences/heatflow/).

References

Aktar, M., Karabulut, H., Özalaybey, S., and Childs, D.: A conjugate strike-slip fault system within the extensional tectonics of Western Turkey, Geophys. J. Int., 171, 1363–1375, 2007.

Aktug, B., Nocquet, J. M., Cingöz, A., Parsons, B., Erkan, Y., England, P., Lenk, O., Gürdal, M. A., Kilicoglu, A., Akdeniz, H., and Tekgül, A.: Deformation of western Turkey from a combination of permanent and campaign GPS data: limits to block-like behavior, J. Geophys. Res., 114, B10404, doi:10.1029/2008JB006000, 2009.

SED

6, 403–426, 2014

Akyol, N., Zhu, L., Mitchell, B. J., Sözbilir, H., and Kekovalı, K.: Crustal structure and local seismicity in western Anatolia, Geophys. J. Int., 166, 1259–1269, 2006.
Balkan, E., Şalk, M., and Erkan, K. : A statistical analysis of thermal conductivity of major rock types in Western Turkey, in preparation, 2014.
Beardsmore, G. R. and Cull, C. P.: Crustal Heat Flow: a Guide to Measurement and Modeling, Cambridge Univ. Press., Cambridge, UK, 2001.
Blackwell, D. D.: Heat flow in the northern basin and range province, the role of heat in the development of energy and mineral resources in the northern basin and range province, Spec. Rep. 13, 81–93, 1983.
Blackwell, D. D. and Spafford, R. E.: Experimental methods in continental heat flow, Methods in Experimental Physics, 24, 189–226, 1987.
Blackwell, D. D. and Steele, J. L.: Thermal conductivity of sedimentary rocks: measurement and significance, in: Thermal History of Sedimentary Basins, Springer, New York, 13–36, 1989.
Blackwell, D. D., Bowen, R. G., Hull, D. A., Ricco, R., and Steele, J. L.: Heat flow, arc volcanism and subduction in Northern Oregon, J. Geophys. Res., 87, 8735–8754, 1982.
Blackwell, D. D., Steele, J. L., Frohme, M. K., Murphey, C. F., Priest, G. R., and Black, G. L.: Heat flow in the Oregon Cascade range and its correlation with regional gravity, Curie point depths, and geology, J. Geophys. Res., 95, 19475–19493, 1990.
Blackwell, D. D., Steele, J. L., and Carter, L. S.: Heat flow patterns of the North American continent: a discussion of the DNAG geothermal map of North America, in: Neotectonics of North America: Geological Society of America DNAG Decade Map, 1, 423–437, 1991.
Bonner, J. L., Blackwell, D. D., and Herrin, E. T.: Thermal constraints on earthquake depths in California, Bull. Seis. Soc. Am., 93, 2333–2354, 2003.
Bozkurt, E.: Neotectonics of Turkey – a synthesis, Geodin. Acta, 14, 3–30, 2001.
Bozkurt, E. and Sozbilir, H: Tectonic evolution of the Gediz Graben: field evidence for an episodic, two-stage extension in western Turkey, Geol. Mag., 141, 63–79, 2004.
Clark, S. P.: Handbook of physical constants, Geol. Soc. Am. Bull., 90, 587 pp., 1966.
Çiftçi, N. B. and Bozkurt, E.: Structural evolution of the Gediz Graben, SW Turkey: temporal and spatial variation of the graben basin, Basin Res., 22, 846–873, 2010.
Erkan, K. and Blackwell, D. D.: A thermal test of the post-subduction tectonic evolution along the California transform margin, Geophys. Res. Lett., 35, L07309, doi:10.1029/2008GL033479, 2008.

Erkan, K. and Blackwell, D. D.: Transient thermal regimes in the Sierra Nevada and Baja California outer arcs following the cessation of Farallon subduction, J. Geophys. Res., 114, B02107, doi:10.1029/2007JB005498, 2009.

Erkan, K., Holdmann, G., Benoit, W., and Blackwell, D.: Understanding the Chena Hot Springs, Alaska, geothermal system using temperature and pressure data from exploration boreholes, Geothermics, 37, 565–585, 2008.

Förster, C. and Smith, L.: The influence of groundwater flow on thermal regimes in mountainous terrain: a model study, J. Geophys. Res., 94, 9439–9451, 1989.

Fytikas, M., Innocenti, F., Manetti, P., Peccerillo, A., Mazzuoli, R., and Villari, L.: Tertiary to Quaternary evolution of volcanism in the Aegean region, Geological Society, London, Special Publications, 17, 687–699, 1984.

Gessner, K., Ring, U., Johnson, C., Hetzel, R., Passchier, C. W., and Güngör, T.: An active bivergent rolling-hinge detachment system: Central Menderes metamorphic core complex in western Turkey, Geology, 29, 611–614, 2001.

Glodny, J. and Hetzel, R.: Precise U-Pb ages of syn-extensional Miocene intrusions in the central Menderes Massif, western Turkey, Geol. Mag., 144, 235–246, doi:10.1017/S0016756806003025, 2007.

İlkışık, O. M., Yalçın, M. N., Sarı, C., Okay, N., Bayrak, M., Öztürk, S., Şener, Ç., Yenigün, H. M., Yemen, H., Sözen, İ., and Karamanderesi, İ. H.: Ege Bölgesi'nde Isı Akısı Araştırmaları, TÜBİTAK Proje No: YDABÇAG-233/G, Ankara, 1996.

İlkışık, O. M., Sarı, C., Bayrak, M., Öztürk, S., Şener, Ç., Yenigün, H. M., and Karamanderesi, İ. H. : Ege Bölgesinde Jeotermik Araştırmalar, TÜBİTAK, Proje No: YDABÇAG-430/G, Ankara, 1997.

Jaeger, J. C.: Application of the theory of heat conduction to geothermal measurements, in: Terrestrial Heat Flow, edited by: Lee, H. K., American Geophysical Union Geophysical Monograph Series No 8, 7–23, 1965.

Jongsma, D.: Heat flow in the Aegean Sea, Geophys. J. Int., 37, 337–346, 1974.

Koçyiğit, A., Yusufoğlu, H., and Bozkurt, E.: Evidence from the Gediz graben for episodic two-stage extension in western Turkey. J. Geol. Soc., 156, 605–616, 1999.

Pfister, M., Ryback, L., and Şimşek, Ş.: Geothermal reconnaissance of the Marmara Sea region (NW Turkey), surface heat flow density in an area of active continental extension, Tectonophysics, 291, 77–89, 1998.

Piromallo, C. and Morelli, A.: *P* wave tomography of the mantle under the Alpine-Mediterranean area, J. Geophys. Res., 108, 2065, doi:10.1029/2002JB001757, 2003.

Ring, U., Johnson, C., Hetzel, R., and Gessner, K.: Tectonic denudation of a Late Cretaceous–Tertiary collisional belt: regionally symmetric cooling patterns and their relation to extensional faults in the Anatolide belt of western Turkey, Geol. Mag., 140, 421–441, 2003.

Roy, R. F., Blackwell, D. D., and Decker, E. R.: Continental Heat Flow, the Nature of the Solid Earth, 506–543, 1972.

Sammel, E. A: Convective flow and its effect on temperature logging in small-diameter wells, Geophysics, 33, 1004–1012, 1968.

Seyitoğlu, G. and Scott, B. C.: Age of the Alaşehir graben (west Turkey) and its tectonic implications, Geol. J., 31, 1–11, 1996.

Seyitoglu, G., Işık, V., and Cemen, I.: Complete Tertiary exhumation history of the Menderes massif, western Turkey: an alternative working hypothesis, Terra Nova, 16, 358–364, 2004.

Tester, J. W., Anderson, B., Batchelor, A., Blackwell, D., DiPippo, R., Drake, E., Garnish, J., Livesay, B., Moore, M. J., Nichols, K., Petty, S., Toksöz, M. N., Veatch Jr, R. W., Baria, R., Augustine C., Enda, M., Negraru, P., and Richards, M.: The Future of Geothermal Energy: Impact of Enhanced Geothermal Systems (EGS) on the United States in the 21st Century, Massachusetts Institute of Technology, 358 pp., 2006.

Tezcan, A. K. and Turgay, M. I.: Heat flow and temperature distribution in Turkey, in: Geothermal Atlas of Europe, edited by: Cermak, V., Haenal, R., and Zui, V., 84–85, 1991.

Thakur, M., Blackwell, D. D., and Erkan, K.: The regional thermal regime in Dixie Valley, Nevada, USA, Geoth. Res. T., 36, 59–67, 2012.

Wollenberg, H. A. and Smith, A. R.: Radiogenic heat production of crustal rocks: an assessment based on geochemical data, Geophys. Res. Lett., 14, 295–298, 1987.

SED
6, 403–426, 2014

SED
6, 403–426, 2014

Table 1. Data locations, borehole information, calculated gradients (Classes B, C, and D) and heat flow values (classes B and C). See Fig. 1 for administrative province codes; BHT: bottom-hole-temperature; T_0: extrapolated mean annual surface temperature (MAST); G: gradient; Cr. G: gradient after topographic correction; K: thermal conductivity; Q: (Corrected) heat flow.

Name	Lat (Deg.)	Lon (Deg.)	Prov.	Elev. (m)	Depth (m)	BHT (°C)	To (°C)	Interval (m)	G (°C km^{-1})	Cr. G (°C km^{-1})	K[a] (W m^{-1} K^{-1})	Q (mW m^{-2})	Lithology	Class
Pursunler	39.2270	28.2017	BAL	294	86	17.8	15.7	13–82	24.6	28.5	1.96 (M)	56	Andesite	B
Alacaatli	39.2534	28.0488	BAL	262	71	16.1	14.7	0–71	19.7	24.5	2.1 (L)	51	Andesite	C
Akcal	39.6038	27.5416	BAL	250	100	17.3	15.0	0–100	23.0	37.1				D
Cakirca	40.4762	29.6630	BUR	94	124	18.2	14.6	0–124	29.0		1.5 (L)	44	Quat.Aluv.	C
Kursunlu	40.4014	29.1105	BUR	15	72	16.7	14.7	50–70	30.0		1.5 (L)	45	Quat.Aluv.	C
Kite	40.1972	28.8763	BUR	74	156	20.1	15.3	20–148	32.5		1.5 (L)	49	Quat.Aluv.	C
As.Vet.	40.3980	29.0986	BUR	11	40	16.6	14.7	24–38	47.5		1.5 (L)	71	Quat.Aluv.	D
Yapildak	40.2005	26.5561	CAN	140	70	18.6		27–65	76.3	85.3	1.0 (L)	85	Mudstone	B
Intepe	40.0279	26.3434	CAN	151	127	24.9	15.7	69–124	42.6	43.6	2.1 (L)	92	Diabase	B
Terzialan	39.9565	27.0234	CAN	152	83	17.2	14.0	17–73	41.1		1.0 (L)	41	Mudstone	C
Cavuskoy	40.2480	27.2407	CAN	21	162	21.8	16.3	125–162	32.4		1.5 (L)	49	Quat.Aluv.	C
Pazarkoy	39.8647	27.3855	CAN	162	88	17.8	13.2	15–82	50.7		1.5 (L)	76	Quat.Aluv.	C
Ovaciki	38.2898	26.7599	IZM	137	106	20.5	16.4	46–106	38.3	49.0	1.73 (M)	85	Marl	B
Ciftlikkoy	38.2879	26.2796	IZM	51	98	22.5	17.2	32–74	50.0		1.73 (M)	86	Marl	B
Yenmis	38.4597	27.4172	IZM	189	88	18.7	15.9	48–82	35.3		1.5 (L)	53	Quat.Aluv.[b]	C
Yusufdere	38.2172	27.8396	IZM	128	90	17.8	14.8	52–88	38.9	33.6	1.5 (L)	50	Quat.Aluv.[b]	C
Bademli	38.0500	28.0792	IZM		90	16.5	14.7	20–90	21.4		4.05 (M)	87	Sandstone	C
Gumuskoy	39.4882	29.7627	KUT	1037	156	17.2	11.7	28–89	34.5					D
Sapcidede	39.5884	29.3348	KUT	1014	74	14.9	11.7	36–74	40.3					D
Koprucek	39.3660	29.3349	KUT	1046	158	14.5		100–150	26.8	27.7				D
Darica	39.6380	29.8707	KUT	1165	90	15.9	11.3	40–78	50.3					D
Y.Armutcuk	39.1200	29.6700	KUT	1213	122	15.6	12.0	0–122	29.2					D
Alahidir	38.5000	27.8974	MAN	145	182	25.8	19.0	114–182	36.8		1.5 (L)	55	Quat.Aluv.[b]	C
Kizilavlu	38.5649	28.3404	MAN	289	110	23.3	17.4	70–110	52.5		1.5 (L)	79	Quat.Aluv.	C
Cataloluk	38.8943	28.4907	MAN	676	122	21.5	15.8	90–122	25.0		3.5 (L)	88	Sandstone	C
K.Belen	38.7500	27.2583	MAN	370	74	26.2	18.7	0–66	57.6		1.8 (L)	104	Andesite	C
Ibrahimaga	38.6284	28.6784	MAN	509	152	20.3	16.6	28–64	55.6		2.42 (M)	134	Schist	C
Boyali	38.8338	28.1418	MAN	502	104	21.5	17.3	20–104	40.5					D
Gumuskol	38.4627	29.1657	USA	895	230	27.3	15.0	19–108	52.1					D
Balabanci	38.3618	28.9149	USA	716	92	18.8	15.8	20–50	38.0					D
Karlik	38.7001	29.5954	USA	1066	120	17.3	12.7	34–104	42.3					D
Karakuyu	38.7680	29.1116	USA	789	114	20.4	14.3	0–108	56.1					D
Beylerhan	38.7000	29.2100	USA	627	118	18.4	14.5	38–68	56.3					D
Salmanlar	38.5600	29.5700	USA	925	56	16.5	14.0	44–52	52.0					D

[a] M: Measured ; L: Literature (Balkan et al., 2014; Blackwell and Steele, 1989; Clark, 1966)
[b] Site is located on an alluvial fan.

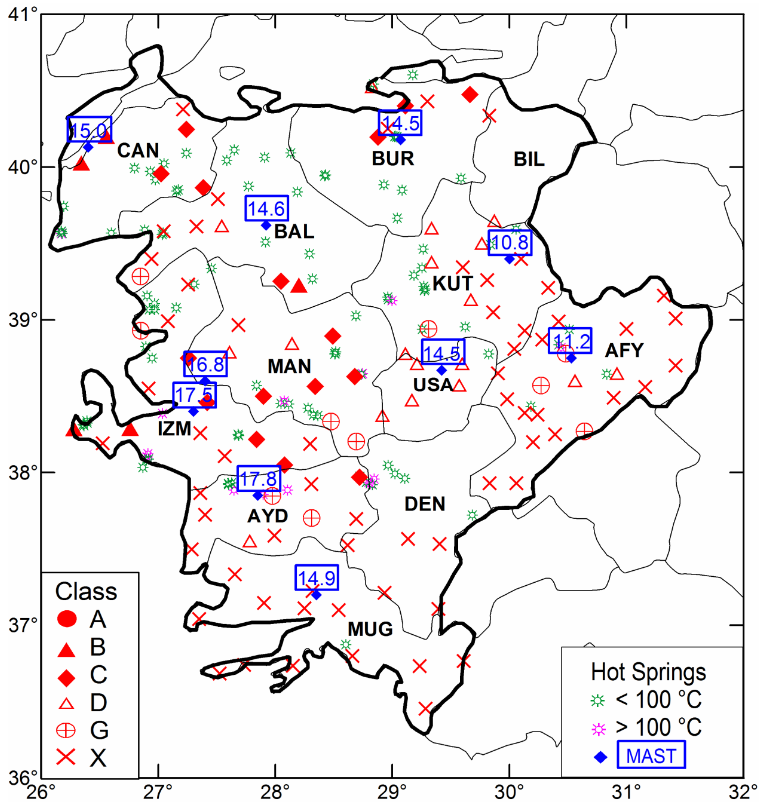

Fig. 1. Regional distribution of the borehole data used in this study. The quality classes are shown by different symbols (see the text for class definitions). Mean Annual Surface Temperatures (MAST) values for each province were obtained from Royal Netherlands Meteorological Institute (KNMI) database (www.knmi.nl). Letter codes for provinces (CAN: Canakkale; BAL: Balı kesir; BUR: Bursa; BIL: Bilecik; KUT: Kütahya; MAN: Manisa; USA: Uşak; AFY: Afyon; IZM: Izmir; DEN: Denizli; AYD: Aydı n; MUG: Muğla).

SED
6, 403–426, 2014

Crustal heat flow measurements in western Anatolia

K. Erkan

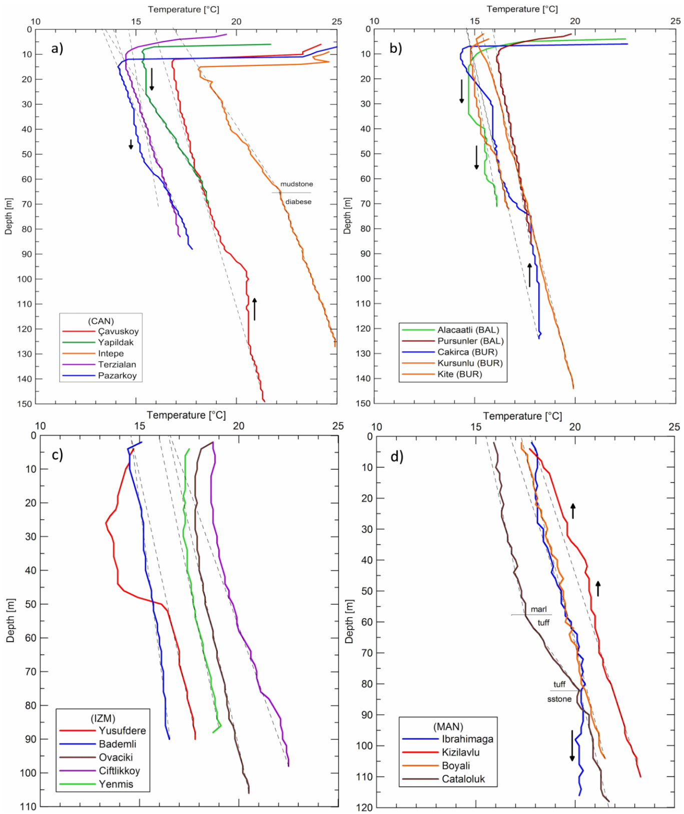

Fig. 2. Temperature-depth (T-D) curves for classes B and C data for provinces of **(a)** Çanakkale **(b)** Balıkesir and Bursa **(c)** Izmir, and **(d)** Manisa. Vertical arrows indicate the inferred direction of intra-borehole fluid flow. The dashed lines represent the undisturbed formation temperatures.

SED
6, 403–426, 2014

Crustal heat flow measurements in western Anatolia

K. Erkan

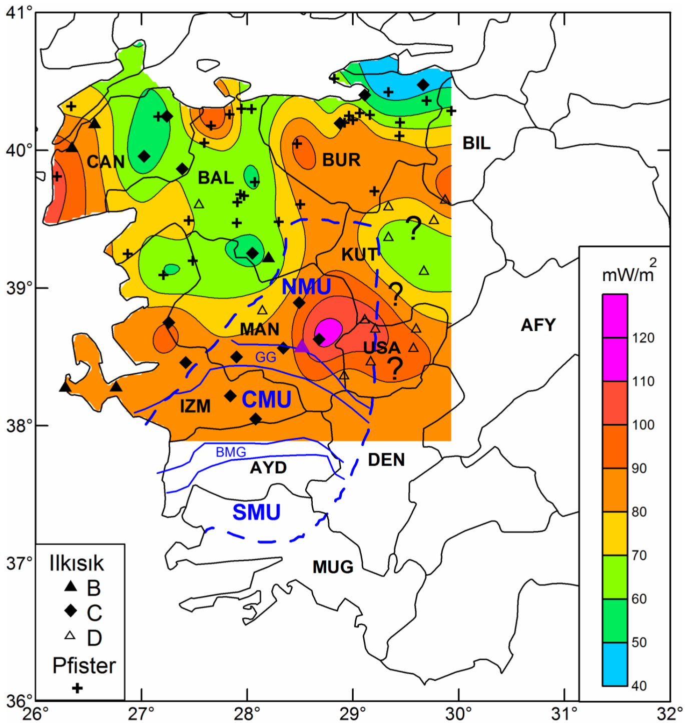

Fig. 3. The map of crustal heat flow in western Anatolia, Turkey based on the data from this study (Table 1), and the data reported by Pfister et al. (1998). Blue lines outline the boundary of the Menderes horst-graben system. GG: Gediz Graben; BMG: Büyük Menderes Graben; NMU: Northern Menderes Unit; CMU: Central Menderes Unit; SMU: Southern Menderes Unit. For provinces of KUT and USA countering is based Class D type data (generic value of K = 2.0 $\mathrm{W\,m^{-1}\,K^{-1}}$) so the map has unknown reliability in these provinces. Location of Kula volcanic field is shown by a purple triangle.

SED
6, 403–426, 2014

Crustal heat flow measurements in western Anatolia

K. Erkan

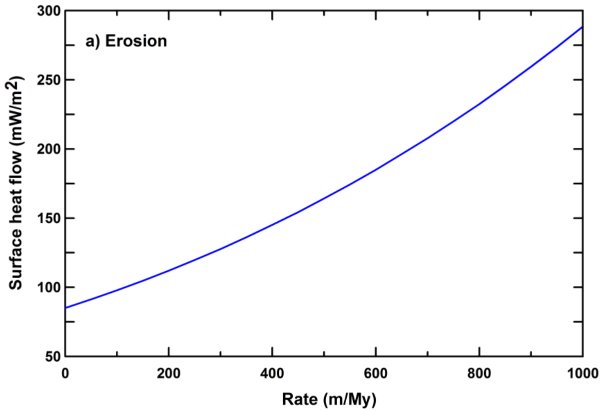

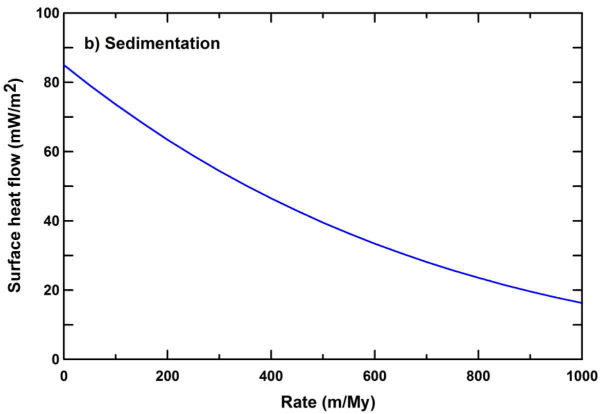

Fig. 4. Surface heat flow for increasing rates of **(a)** erosion and **(b)** sedimentation. These models were generated assuming erosion/sedimentation activity for the last 5 Myr, a background heat flow of 85 $mW\,m^{-2}$, and thermal diffusivity of $1 \times 10^{-7}\,m^2\,s^{-1}$.

SED
6, 403–426, 2014

Crustal heat flow measurements in western Anatolia

K. Erkan

Title Page
Abstract Introduction
Conclusions References
Tables Figures
◀ ▶
Back Close
Full Screen / Esc
Printer-friendly Version
Interactive Discussion